Predictive Effect of Spatial Protein Signature in Advanced Non-small Cell Lung Cancer Patients Treated with Bispecific Antibody (KN046) Immunotherapy

Xinyu Song (sdsxydu@163.com)
Tongji University

Anwen Xiong
Shanghai Pulmonary Hospital

Tao Jiang
Shanghai Pulmonary Hospital

Peixin Chen
Tongji University

Xuefei Li
Shanghai Pulmonary Hospital

Fengying Wu
Shanghai Pulmonary Hospital

Xiaoshen Zhang
Tongji University

Zhikai Zhao
Shanghai Pulmonary Hospital

Lei Cheng
Shanghai Pulmonary Hospital

Chao Zhao
Shanghai Pulmonary Hospital

Zhehai Wang
Shandong Cancer Hospital

Dawei Chen
Shandong Cancer Hospital

Xiaoqian Wu
Yucebio

Shengqiang Xu
Yucebio

Ting Xu
Alphamab Biopharmaceuticals

Xiaofan Su
Yucebio
Caicun Zhou
Shanghai Pulmonary Hospital

Research Article

Keywords: DSP, immunotherapy, KN046, NSCLC, predictive signature

Posted Date: April 15th, 2022

DOI: https://doi.org/10.21203/rs.3.rs-1553755/v1

Abstract

Background

Immunotherapy, targeting programmed death ligand-1 (PD-L1) and cytotoxic T lymphocyte-associated antigen-4, has shown significant antitumor activity and favourable safety profile in patients with advanced non-small cell lung cancer (NSCLC), while predictive biomarkers remain largely unknown. Here, we investigated the predictive effect of spatial protein expression signature of KN046, a bispecific antibody (bsAb), as a treatment in advanced NSCLC patients.

Methods

Digital spatial profiling was used to investigate protein expression in both tumor and stroma areas of formalin-fixed paraffin-embedded sections at baseline. Regions of interests (ROIs) were recorded after tricolor fluorescence labeling. The geometric means of different protein expression of different response groups were combined to construct the tumor signature, the stroma signature and the tumor + stroma signature. The accurate score was determined by receiver operating characteristic curve and the area under the curve (AUC).

Results

Eight patients with partial response (PR) and nine with progressive disease (PD) were enrolled in the study. Among 133 ROIs, 14 proteins expressed differently between PR and PD groups (both $P < 0.05$). Among tumor areas, tumor necrosis factor superfamily member 4, CD276, B-cell lymphoma-2 and CD45RO were highly expressed in PR group, while transmembrane protein 173 was highly expressed in PD group (both $P < 0.05$). Among stroma areas, PR group exhibited a greater expression of T cell immunoglobulin and mucin domain 3 (Tim-3), PD-L1, complement component 3 receptor 4 subunit (CD11c) and Beta-2-microglobulin (B2M) than those in PD group ($P < 0.05$). The stroma signature showed a superior predictive performance (AUC = 0.840, $P < 0.05$) to the tumor + stroma signature (AUC = 0.732, $P < 0.05$) and the tumor signature (AUC = 0.670, $P < 0.05$). The predictive effect of the stroma signature was much better than that of PD-L1 expression or tumor mutation burden.

Conclusions

In NSCLC, we firstly found that there are differences in the expression of immune-related proteins in different spatial regions. And we successfully developed a stroma signature with Tim-3/PD-L1/CD11c/B2M which could better predict the response to KN046. This signature might potentially complement the limitations of PD-L1 and TMB measurements and be useful in clinical practice about bsAbs.

Introduction

Non-small cell lung cancer (NSCLC) is a frequently occurring malignancy and is one of the main causes of cancer-related deaths worldwide. At diagnosis, many patients already have advanced stage disease with an unfavorable prognosis.[1] Immunotherapy that targets the programmed death-1 (PD-1)/programmed death ligand-1 (PD-L1) pathway, has changed the treatment landscapes of advanced NSCLC and markedly increased overall survival. However, immunotherapy is still confronted with many challenges, particularly in overcoming drug resistance, identifying accurate biomarkers, and managing immune-related adverse events (irAEs).[2–6]

Several studies have explored the combination of two different immunotherapeutic drugs with the aim of improving the efficacy of immunotherapy. PD-1/PD-L1 and cytotoxic T lymphocyte-associated antigen-4 (CTLA-4) are two of the classic immune targets and immunotherapy aimed to target them simultaneously is rapidly developing.[7–11] KN046 is a bispecific antibody (bsAb) targeting PD-L1 and CTLA-4.[12] The safety and clinical effectiveness of KN046 in advanced NSCLC patients were evaluated in a phase 2, multicenter clinical study (NCT03838848). The median progression-free survival (mPFS) with KN046 in second or beyond line therapy was 3.7 months in intention-to-treat population. PFS in squamous NSCLC patients were 7.3 months, showing a benefit advantage compared with the historical data of PD-1/PD-L1 monotherapy.[13] But the biomarkers of efficacy remains unclear.

In advanced NSCLC patients, acquisition of tissue remains a key issue. Biopsy through bronchoscopy or CT guided transthoracic core needle biopsy is frequently performed to get tissue samples. We hope to extract as much information as possible from limited biopsy specimens. Traditional immunohistochemical (IHC) allows spatial analysis of tumor cells, but the amount of available information is limited.[14, 15] This method only measures 3–4 targets at a time and it can not characterize actual cell proportions, cell heterogeneity, or deeper spatial distributions.[16] In recent years, great progress has made in multiple to single-cell sequencing, but the spatial location information could not be obtained. The application of formalin fixed paraffin embedding (FFPE) in biopsy specimens is strictly limited because most of the emerging sequencing methods have high requirements on specimen freshness and size.[17, 18] These limitations could be potentially eliminated with the development of space multi-target technology. NanoString Biotechnology's digital spatial profiling (DSP) is a next-generation spatial multi-target analysis system. It is a state of the art platform that combines fluorescence, IHC, and transcriptome techniques to achieve high throughput, multiomics and elastic selection of region of interest (ROI). It provides more comprehensive and clear biological images, thus collecting spatially morphological information and multiple expression data which could not be obtained simultaneously through traditional analysis platforms.

In the study, we retrospectively collected 17 specimens from the different response groups in a phase II clinical trial of KN046 in advanced NSCLC subjects. DSP of Nano-String GeoMX was used to measure the specific expression of 44 immune cell and immunotherapy related proteins to evaluate the tissue

microenvironment and tumor cells in the two groups of patients and to investigate significant biomarkers for constructing predictive signatures.

Materials And Methods

Sample selection

We collected tissue specimens from patients with advanced NSCLC who were undergoing treatment with KN046 during a phase 2 multicenter study.[13] The inclusion criteria were: aged between 18 and 75 years old; had stage IV NSCLC confirmed by histology or pathology; had negative epidermal growth factor receptor mutation or anaplastic lymphoma kinase rearrangement; and failed or not tolerated to first-line platinum-based chemotherapy. Enrolled patients were given KN046 (3 mg/kg or 5 mg/kg) intravenously every 14 days up to disease progression or intolerable toxicity. Tumor response was evaluated per response evaluation criteria in solid tumours (RECIST) version 1.1.[19]

Procedures of DSP

We followed published experimental methods with modifications as noted below.[20, 21] Briefly, FFPE sections (4μm) of 17 specimens (8 PR and 9 PD) were prepared. Slides were baked at 60°C for 1.5h, then deparaffinized, rehydrated, antigen-retrieved in pressure cooker for 10 minutes at 100°C. For protein detection, UV-photocleavable barcode-conjugated protein probe set (Immune Cell Profiling Core, IO Drug Target Module, Immune Cell Typing Module, and Pan-Tumor Module) and morphology markers (panCK and CD45) were hybridized with the slides at 4℃ overnight, followed by washing with tris buffered saline tween for 3 times to remove off-target probes, then counterstained with nucleus dye (SYTO13) for 15 minutes at room temperature. The morphology markers and nucleus stain allow delineation of the epithelial, immune compartments, and nuclei, respectively. The protein profiling reagents contained 44 targets (**Supplementary Table 1**).

ROI selection were performed on the the immunofluorescence images. Compartment-specific areas of interests (AOIs) were assigned from sequential mask as the stroma (panCK negative staining, tumor-inverse segment) and tumor (panCK positive staining, tumor-enriched segment) compartments. 6–20 AOIs per sample were selected for analysis. The spatially-indexed barcode cleavage and collection were performed on a GeoMx Digital Spatial Profiling instrument (NanoString). The barcodes collected from each AOI were quantitated by the nCounter FLEX (Nanotring), then mapped back to original ROI locations to integrate spatial information with protein expression for individual ROI.

Quality control of the protein data was performed using an nCounter Assay which included 6 positive probes and 6 negative control probes. The content of quality control contains the efficiency of hybridization, purification and imaging. Raw digital counts from the barcodes corresponding to particular probes were normalized. Housekeeping proteins (ribosomal protein S6, histone H3), 2 mouse and rabbit IgGs (negative controls) were employed for further housekeeping and signal-to-noise normalizations. The size of different ROIs was adjusted by area normalization and different cell numbers to avoid variations

across ROIs. By comparing the fluorescence images with the corresponding HE staining (Fig. 1A), each ROIs were spatially identified in the whole tissue. After segmentation, approximately 3–20 AOIs were chosen per specimen according to morphology (Fig. 1B). Finally, up to 133 ROI data were pooled (including 89 tumor areas and 44 stroma areas) and sequenced using NextSeq High Output (ver. 2.5; 75 cycles, 2 × 38 bp; Illumina). All AOIs were quantified by NGS technology.

PD-L1 testing

PD-L1 quantitative detection was followed by the DSP protocol above. The PD-L1 expression was measured though the immune cell profiling core panel. Meanwhile, we also detected PD-L1 expression through traditional automatic IHC. Prepared FFPE sections were put into Ventana BenchMark XT automatic immunohistochemical staining instrument platform (Ventana PD-L1 SP263). The expression was evaluated according to the coloring ratio. PD-L1 positivity was defined according to the tumor proportion score (TPS) staining on tissue: <1% (negative), 1–49% (weak positive), and ≥ 50% (strong positive).

TMB analysis

TMB refered to the total number of somatic mutations with replacement, insertion and deletion per megabyte base in the exon coding region of the genome in a tumor sample. First, tumor samples were extracted from FFPE for DNA isolation and sequencing of genomic DNA. DNA fragments of 200bp to 400bp were isolated from the tissue after shearing, and DNA libraries were constructed using KAPA Hyper Prep kits. Then, the prepared library was hybridized with two different hybridization reagents and blockers in the SureSelectXT Target Enrichment System. Then the enrichment library was amplified with P5/P7 primers. Finally, the library was sequenced on NovaSeq6000 platform (Illumina) after being identified by 2200 bioanalyzer and quantified by Qbit3 and QPCR NGS library quantitative kits. The panel of 825 cancer-related genes were compared with an average coverage depth of more than 700 (Genetron Health, Beijing, China). TMB = number of mutations/panel size (mut/Mb).

Public database validation

The first step of validation was to find the corresponding gene name of the proteins involved in three signatures in the original data set, then screen the gene expression levels of all samples in several external data sets of immunotherapy.[22–26] The average expression of each signature in external data sets samples was calculated as the signature score. Median score was used as the cut off value to divide the samples into high score and low score groups, and to calculate whether the samples could predict efficacy. According to the response of patients, complete response (CR) and partial response (PR) were divided into response group, pregressive disease (PD) and stable diease (SD) were non-response group. Wilcox statistical analysis and receiver operating characteristic (ROC) analysis were used to evaluate whether signature score could accurately predict efficacy.

Statistical analysis

All data were corrected by Benjamini–Hochberg (BH) method, which controlled the false discovery rate by utilizing the sequential modified Bonferroni correction for the testing of multiple hypotheses.[27] The formula employed as: *P *(m/k)*; where the common *P*-value is *P*, the number of tests is *m;* and the *P*-value ranking for this test among all tests is *k*. After correction, the geometric means of different proteins between 2 groups ($P < 0.01$) made up a signature [*Σ(log2(Xi + 1))/N*; *Xi* was the normalized expression value of each protein, *N* was the number of proteins included in the signature].

For expression data analysis, when multiple probes were available, outlier probes were deleted from each target and expression values evaluated as geometric means of remaining probes. The deduplicated count value was used to report single probe genes. The limit of quantitation was the geometric mean of the negative control probes + 2 geometric standard deviations of the negative control probes. Upper quartile (Q3) normalization was applied to each set of data.

ROC curves of the signature were drawn and area under the curve (AUC) were calculated to show the predictive effects of a signature. In a binary classifier, a ROC curve can be used to estimate the tradeoffs between sensitivity and specificity. The result yields a plot of the true positive rate (TPR, or specificity) *vs* the false positive rate (FPR, or 1-sensitivity). After the curve was drawn, a qualitative analysis of the signature was performed. If the signature was to be quantitatively analyzed, AUC calculation was needed. Obviously, the larger the AUC, the better the predictive effect. The closer the AUC is to 1.0, the higher the authenticity of a method and the greater of the predictive value.

Results

Patient and sample characteristics

A total of 41 patients were screened. 20 patients obtained PR or PD after treatment. Among them, 4 had unqualified FFPE slides. Finally, 17 were enrolled, with 8 patients in PR and 9 in PD groups, respectively (Fig. 2). Median age was 61.8 years with 88.2% (15/17) of men and 23.5% (4/17) of never smokers. The majority of patients had ECOG performance status 1 (16/17, 94.1%), adenocarcinoma (11/17, 64.7%), negative PD-L1 expression (12/17, 70.6%), and TMB level ≥ 10 mut/Mb (13/17, 76.5%). All patients progressed after first-line platinum-based chemotherapy. There were no statistical difference in demographic or baseline characteristics between the two groups (Table 1).

Spatial protein information

Forty-four proteins detected by DSP including immune cell profiles, immuno-oncology drug targets, immune cell typing, and pan-tumor panels. Protein information of patients was clustered according to different therapeutic effects. Heat map suggested that proteins in different areas had different expression between two groups. When protein expression was plotted in boxplot after BH test, the expression of CD276 (B7-H3) ($P = 0.0001$), CD45RO ($P = 0.0002$), B-cell lymphoma-2 (Bcl-2) ($P = 0.0003$), PD-L1 ($P = 0.0006$), CD14 ($P = 0.0013$), tumor necrosis factor receptor superfamily member 18 (GITR) ($P = 0.0014$), phosphatase and tensin homolog (PTEN) ($P = 0.0018$), progesterone receptor (P = 0.0027), fibroblast

activation protein alpha (FAP-alpha) (P = 0.0081), complement component 3 receptor 4 subunit (CD11c) (P = 0.0071), CD45 (P = 0.0097), CD34 (P = 0.0098), and tumor necrosis factor superfamily member 4 (OX40L) (P = 4.8e-05) were significantly higher in PR group, while transmembrane protein 173 (STING) (P = 0.0007) were higher in PD group. In tumor areas, OX40L (P = 0.0002), B7-H3 (P = 0.0007), Bcl-2 (P = 0.0008), and CD45RO (P = 0.0031) were significantly highly expressed but STING (P = 3.5e-05) was lowly expressed in PR group. In stroma areas, expression levels of T cell immunoglobulin and mucin domain 3 (Tim-3) (P = 0.0028), PD-L1 (P = 0.0030), CD11c (P = 0.0039), and beta-2-microglobulin (B2M) (P = 0.0042) were greater in PR group (Fig. 3). Differential proteins in each part were summarized in **Table 2**.

Construction of predicting response signature

As expected, different areas showed different protein expressions. We constructed signatures to evaluate the predictive value of proteins from different areas. In all areas, the P-value of different proteins between two groups was 6.4e-06, the AUC of tumor + stroma signature was 0.732. In tumor areas, the P-value was 0.0073, and the AUC of tumor signature was 0.670. In stroma areas, the P-value was 0.0002, and the AUC of stroma signature was 0.840 (Fig. 4). As shown in AUC results, the stroma signature demonstrated the best predictive performance.

Relationship between PD-L1 and clinical efficacy

We used DSP platform to quantitatively detect the expression of PD-L1 in different spatial areas. High expression of PD-L1 was associated with better response to KN046. The expression in all areas, tumor areas and stroma areas were all higher in PR group than in PD groups (P = 0.0005, 0.0230, 0.0037, respectively). (Fig. 5) The different PD-L1 expression in different areas suggested the spatial heterogeneity of PD-L1 expression. DSP might be a more accurate methodin detection of PD-L1 expression than traditional IHC.

Relationship between TMB and clinical efficacy

Among 17 patients, 3 of them from PR group had unqualified extraction, and only 1 from PD group had low TMB (< 10 mut/Mb), the other 13 patients all had high TMB (≥ 10 mut/Mb). So there were no statistical significance between PR and PD group (P-value = 0.87). Moreover, due to the small sample size, we were unable to conclude the relationship between TMB level and the response to KN046 (P = 0.89). (Fig. 5)

Comparison with traditional markers

PD-L1 and TMB were common predictive biomarkers for efficacy of immuneotherapy in advanced NSCLC patients. So we compared their AUC values with our signatures. In all areas, the AUC of PD-L1 was 0.678, the AUC of TMB was 0.533, which were significantly lower than our signature (AUC = 0.732) in all areas. In tumor areas, the AUC of PD-L1 was 0.643, suggested that the tumor signature (AUC = 0.670) can better predict the response of KN046. In stroma areas, the AUC of PD-L1 was 0.761, also showing our stroma signature (AUC = 0.840) had a better performance than tumor PD-L1 or TMB in predicting the efficacy of

KN046. (Fig. 5) Therefore, our signatures had better predictive value than traditional biomarkers such as PD-L1 and TMB in all regions.

Public database validated the above signatures

After preliminary screening, further validation sets of 5 classic cancer types treated with PD-1 or CTLA-4 blockade, of which the RNA-sequencing data was available, were selected as validation cohorts.[22–26] We verified the relationship between our three signatures and the effection of immunotherapy respectively. Since the patients in above cohorts not only included NSCLC but also other types of cancer such as head and neck squamous cell carcinoma, melanoma and clear cell renal cell carcinoma, and these patients who were treated with immune monotherapy had data of RNAseq only, we did not establish the relationship between the relevant gene signatures and the efficacy of immunotherapy. (**Supplementary Fig. 1**) To sum up, our protein signature of these predictors might specifically predict the efficacy of KN046 in NSCLC patients.

Discussion

In recent years, immunotherapy has changed the treatment landscapes of lung cancer and prolonged survival of patients. However, PD-1 or PD-L1 monoclonal antibodies have limited efficacy, about 20% of NSCLC patients could get tumor response to immunotherapy.[28] BsAbs can simultaneously target two different checkpoints, which may improve efficacy of immunotherapy and become a promising innovative therapy for cancer patients.[29] KN046 is a BsAb targeting PD-L1 and CTLA4, demonstrating efficacy in 2nd line or beyond treatment of advanced NSCLC patients in the phase II trial.[13] However, its predictive biomarkers are largely unknown. This study demostrated stroma signature based on protein expression is associated with better efficacy of the compound.

Combination of PD-1/PD-L1 and CTLA4 antibodies is synergistic in antitumor effect. The efficacy of this dual immune combination strategy was firstly demonstrated in melanoma patients.[30] In NSCLC, CheckMate227 study suggested that patients could benefit from dual immunotherapy.[31] In CheckMate9LA, overall survival (OS) of nivolumab and ipilimumab and 2 cycles chemotherapy was higher than chemotherapy alone. But the combination of nivolimab and ipilimumab produces significant toxicity, which is mainly due to ipilimumab.[32] Several bsAbs against PD-1/PD-L1 and CTLA4 with the purpose to decrease toxicity of the combination while keep efficacy are being tested.[13, 33, 34] Just like previous PD-L1 or PD-1 inhibitors, not all patients benefit from bsAbs. Up to now, there was no good biomarkers to screen out effective population of bsAbs.

In the process of exploring tumor biomarkers of PD-1/PD-L1 monoclonal antibodies in the past, several biomarkers related to immunotherapy efficacy were found, but all had their limitations. PD-L1 was the most widely used predictor so far. Many studies have noted that patients with higher PD-L1 expression could benefit from immunotherapy, they can achieve longer PFS or OS.[35–38] Another common biomarker is TMB. Several studies revealed that patients with higher TMB had higher objective response rate (ORR)

and longer PFS.[39–41] TMB is closely related to DNA repair defects. Generally, patients with high TMB often have high DNA mismatch repair (dMMR) and high microsatellite instability (MSI-H). A large number of studies have confirmed that patients with advanced solid tumors of MSI-H/dMMR are more likely to benefit from immunotherapy, regardless of cancer type.[42, 43] Tumor infiltrating lymphocytes (TILs), as a kind of highly heterogeneous immune cells, has been shown to be a favorable prognostic factor for many solid tumors, including lung cancer.[44] Precious studies suggested that intense TILs were independent prognostic variable for PFS and OS.[45–47] But the lack of globally consistent criteria and cutpoints may reduce their predictive value. Interferon gamma (IFNγ) related signaling pathways play an important role in exerting anti-tumor immune effects. Patients with high baseline IFN-γ mRNA expression may have longer PFS and OS.[48, 49] However, IFN-related studies mainly focused on melanoma, and data on NSCLC are limited. Then several studies also focused on the relationship between the combination of PD-L1 + TMB and the efficacy of immunotherapy. In CheckMate 568, patients with high TMB + negative PD-L1 showed higher ORR than those with high TMB + positive PD-L1.[50] On the contrary, CheckMate 026 suggested that in PD-L1 positive + high TMB subgroup, the response rate was up to 75%, which was higher than only one factors.[51] Therefore, whether the combination of biomarkers can predict the curative effect remains to be further explored. We need a more advanced platform to access more information about tumor tissue.

DSP technology solved the problem of spatial information detection. The main advantages of DSP was the high reuse capability for FFPE samples, the low operating time, and the non-destructive direct process to define biomarkers in a discrete ROI.[20, 21, 52] In the field of immunotherapy companion diagnostics, Gupta S. et al. and Zugazagoitia J. et al. have confirmed that DSP seems to have quantitative potential compared to IHC, and the technology has the capability to do concomitant diagnostic tests for immunotherapy.[53, 54] DSP was also used in finding biomarkers. It was shown fisrstly to successfully identify 20 biomarkers in melanoma patients, where the expression of PD-L1 in CD68-positive cells rather than tumor cells was an important factor in determining PFS, OS, and treatment response.[55] DSP seems to have the potential to become an accurate technique for determining therapy prognosis after immunotherapy, so we used it to detect prognostic biomarkers from bsAbs.

The composition of tumor microenvironment (TME) plays an important role in inhibiting or enhancing immune response. Tumor stroma is an important part of tumor microenvironment, which plays an important roal of tumor genesis, development and metastasis.[56] The precision of tumor immunotherapy and the exploration of biomarkers should not only focus on tumor cells, but also the stroma information around them and the spatial information of each component should not be ignored. This study firstly validated the immune components and protein expressions in different tumor areas and stroma areas were significantly different using DSP, which also laid a foundation for us to determine more accurate biomarkers. In provious study about NSCLC patients treated with dual immunotherapy combination, CheckMate227 suggested that nivolumab plus ipilimumab improved PFS in patients with high TMB (≥ 10), and prolonged OS in patients with positive PD-L1 expression (≥ 1%).[31, 57] When researches made a combination of these two biomarkers, patients with high TMB + positive PD-L1 achieved longer PFS, but

did not increase PFS when compared to the high TMB + negative PD-L1 subgroup.[31] The combination of PD-L1 and TMB may not make sense. But in our study, we identified a predictive signature of Tim-3, PD-L1, CD11c, and B2M in stroma areas with higher prediction score than tumor cells. Its score exceeded traditional biomarkers PD-L1 and TMB. This suggests that bsAbs immunotherapy may alter the TME and induce greater changes in protein expression of stroma regions. This combination of spatial different proteins may ameliorate some drawbacks of traditional biomarkers. It also provide new method and idea for the exploration of efficacy predictive biomarkers of other bsAb drugs.

Despite our foundings above, this study also had its limitations. When we verified the relative genes and signatures in common database, we were unable to obtain positive results. It may be caused by the following reasons. First, The validation sets focused on multiple cancer types with immune monotherapy, which is different from our target population and treatment regimen. Second, we could only got data at RNA level, it was different from the protein level. Besides, because of the novelty of KN046, relative data can not be obtained from public database. Furthermore, the sample size was small and involved one single center, and due to the amount of collected tissue, we only carried out DSP for protein detection. So our signature of bsAb-KN046 needs to be further validated in subsequent prospective studies and clinical trials involving multiple centers. And in the future, we plan to add other techniques such as single-cell sequencing and spatial transcriptome sequencing to further verify our findings.

In conclusion, our study suggest that there are differences in the expression of immune-related protein information in different spatial regions of tumor tissue, and the signature in stroma region with Tim-3, PD-L1, CD11c, and B2M can better predict the response of a bsAb drug KN046.

Declarations

Ethics approval and consent to participate

Studies involving human participants were reviewed and approved by the Ethics Committee of Shanghai Pulmonary Hospital. The patient/participant provided written informed consent to participate in the study.

Consent for publication

Not applicable.

Availability of data and materials

The datasets used and/or analysed during the current study are available from the corresponding author on reasonable request.

Competing interests

The authors declare that they have no competing interests.

Funding

This work was supported by Shanghai Pulmonary Hospital Innovation Research Group Project (FKCX1903), Science and Technology Innovation Action Plan of Shanghai Science and Technology Commission (19411950300), and Shanghai Collaborative Innovation Project (2020CXJQ02).

Authors' contributions

SXY was a major contributor in writing the manuscript. SXY, XAW, and WXQ assisted in clinical data collection and collation. SXY, ZZK, CL, and ZC were responsible for tissue sample extraction and FFPE production. ZXS analyzed and interpreted the patient data. JT, CPX, LXF, WFY, WZH, CDW and XT performed the construction of ideas and revision of articles. XSQ and SXF offered technical support. ZCC oversaw the whole process as the corresponding author, . All authors read and approved the final manuscript.

Acknowledgements

Not applicable.

References

1. Cao W, Chen HD, Yu YW, et al. Changing profiles of cancer burden worldwide and in China: a secondary analysis of the global cancer statistics 2020. Chin Med J (Engl) 2021;134:783–791.
2. Schreiber RD, Old LJ, Smyth MJ. Cancer immunoediting: integrating immunity's roles in cancer suppression and promotion. Science 2011;331:1565–1570.
3. Azoury SC, Straughan DM, Shukla V. Immune Checkpoint Inhibitors for Cancer Therapy: Clinical Efficacy and Safety. Curr Cancer Drug Targets 2015;15:452–462.
4. Topalian SL, Hodi FS, Brahmer JR, et al. Safety, activity, and immune correlates of anti-PD-1 antibody in cancer. N Engl J Med 2012;366:2443–2454.
5. Xia L, Liu Y, Wang Y. PD-1/PD-L1 Blockade Therapy in Advanced Non-Small-Cell Lung Cancer: Current Status and Future Directions. Oncologist 2019;24:S31-S41.
6. Tumeh PC, Harview CL, Yearley JH, et al. PD-1 blockade induces responses by inhibiting adaptive immune resistance. Nature 2014;515:568–571.
7. Snyder A, Makarov V, Merghoub T, et al. Genetic basis for clinical response to CTLA-4 blockade in melanoma. N Engl J Med 2014;371:2189–2199.
8. De Giglio A, Di Federico A, Nuvola G, et al. The Landscape of Immunotherapy in Advanced NSCLC: Driving Beyond PD-1/PD-L1 Inhibitors (CTLA-4, LAG3, IDO, OX40, TIGIT, Vaccines). Curr Oncol Rep 2021;23:126.
9. Lafuente-Sanchis A, Zuniga A, Estors M, et al. Association of PD-1, PD-L1, and CTLA-4 Gene Expression and Clinicopathologic Characteristics in Patients With Non-Small-Cell Lung Cancer. Clin

Lung Cancer 2017;18:e109-e116.
10. Puri S, Shafique M. Combination checkpoint inhibitors for treatment of non-small-cell lung cancer: an update on dual anti-CTLA-4 and anti-PD-1/PD-L1 therapies. Drugs Context 2020;9.
11. Rotte A. Combination of CTLA-4 and PD-1 blockers for treatment of cancer. J Exp Clin Cancer Res 2019;38:255.
12. Ramos-Casals M, Brahmer JR, Callahan MK, et al. Immune-related adverse events of checkpoint inhibitors. Nat Rev Dis Primers 2020;6:38.
13. C. Zhou AX, W. Li, Z. Ma, X. Li, J. Fang, Q. Xie, Y. Fan, J. Xu, H. Van, P. Kong, F. Yang, J. Li, Y. Lu, T. Xu. A Phase II Study of KN046 (Bispecific Anti-PD-L1/CTLA-4) in Patients (pts) with Metastatic Non-Small Cell Lung Cancer (NSCLC). Journal of thoracic oncology 2021;16(3):S636.
14. Ichikawa T, Saruwatari K, Mimaki S, et al. Immunohistochemical and genetic characteristics of lung cancer mimicking organizing pneumonia. Lung Cancer 2017;113:134–139.
15. Kim H, Kwon HJ, Park SY, et al. PD-L1 immunohistochemical assays for assessment of therapeutic strategies involving immune checkpoint inhibitors in non-small cell lung cancer: a comparative study. Oncotarget 2017;8:98524–98532.
16. Yatabe Y, Dacic S, Borczuk AC, et al. Best Practices Recommendations for Diagnostic Immunohistochemistry in Lung Cancer. J Thorac Oncol 2019;14:377–407.
17. Ma KY, Schonnesen AA, Brock A, et al. Single-cell RNA sequencing of lung adenocarcinoma reveals heterogeneity of immune response-related genes. JCI Insight 2019;4.
18. Mathieson W, Marcon N, Antunes L, et al. A Critical Evaluation of the PAXgene Tissue Fixation System: Morphology, Immunohistochemistry, Molecular Biology, and Proteomics. Am J Clin Pathol 2016;146:25–40.
19. Eisenhauer EA, Therasse P, Bogaerts J, et al. New response evaluation criteria in solid tumours: revised RECIST guideline (version 1.1). Eur J Cancer 2009;45:228–247.
20. Merritt CR, Ong GT, Church S, et al. High multiplex, digital spatial profiling of proteins and RNA in fixed tissue using genomic detection methods. 2019.
21. Decalf J, Albert ML, Ziai J. New tools for pathology: a user's review of a highly multiplexed method for in situ analysis of protein and RNA expression in tissue. J Pathol 2019;247:650–661.
22. Prat A, Navarro A, Pare L, et al. Immune-Related Gene Expression Profiling After PD-1 Blockade in Non-Small Cell Lung Carcinoma, Head and Neck Squamous Cell Carcinoma, and Melanoma. Cancer Res 2017;77:3540–3550.
23. Liu D, Schilling B, Liu D, et al. Integrative molecular and clinical modeling of clinical outcomes to PD1 blockade in patients with metastatic melanoma. Nat Med 2019;25:1916–1927.
24. Riaz N, Havel JJ, Makarov V, et al. Tumor and Microenvironment Evolution during Immunotherapy with Nivolumab. Cell 2017;171:934–949 e916.
25. Nathanson T, Ahuja A, Rubinsteyn A, et al. Somatic Mutations and Neoepitope Homology in Melanomas Treated with CTLA-4 Blockade. Cancer Immunol Res 2017;5:84–91.

26. Braun DA, Hou Y, Bakouny Z, et al. Interplay of somatic alterations and immune infiltration modulates response to PD-1 blockade in advanced clear cell renal cell carcinoma. Nat Med 2020;26:909–918.
27. Haynes W. Benjamini–Hochberg Method. In: Dubitzky W, Wolkenhauer O, Cho K-H, et al., eds. *Encyclopedia of Systems Biology*. New York, NY: Springer New York; 2013:78–78.
28. Brahmer JR, Tykodi SS, Chow LQ, et al. Safety and activity of anti-PD-L1 antibody in patients with advanced cancer. N Engl J Med 2012;366:2455–2465.
29. Esfandiari A, Cassidy S, Webster RM. Bispecific antibodies in oncology. Nat Rev Drug Discov 2022.
30. Curran MA, Montalvo W, Yagita H, et al. PD-1 and CTLA-4 combination blockade expands infiltrating T cells and reduces regulatory T and myeloid cells within B16 melanoma tumors. Proc Natl Acad Sci U S A 2010;107:4275–4280.
31. Hellmann MD, Paz-Ares L, Bernabe Caro R, et al. Nivolumab plus Ipilimumab in Advanced Non-Small-Cell Lung Cancer. N Engl J Med 2019;381:2020–2031.
32. Paz-Ares L, Ciuleanu TE, Cobo M, et al. First-line nivolumab plus ipilimumab combined with two cycles of chemotherapy in patients with non-small-cell lung cancer (CheckMate 9LA): an international, randomised, open-label, phase 3 trial. Lancet Oncol 2021;22:198–211.
33. Chen W, Pandey M, Sun H, et al. Development of a mechanism of action-reflective, dual target cell-based reporter bioassay for a bispecific monoclonal antibody targeting human CTLA-4 and PD-1. *MAbs* 2021;13:1914359.
34. Lussier DM, Johnson JL, Hingorani P, et al. Combination immunotherapy with alpha-CTLA-4 and alpha-PD-L1 antibody blockade prevents immune escape and leads to complete control of metastatic osteosarcoma. J Immunother Cancer 2015;3:21.
35. Balar AV, Castellano D, O'Donnell PH, et al. First-line pembrolizumab in cisplatin-ineligible patients with locally advanced and unresectable or metastatic urothelial cancer (KEYNOTE-052): a multicentre, single-arm, phase 2 study. Lancet Oncol 2017;18:1483–1492.
36. Aggarwal; Leora Horn; Amita Patnaik; Matthew Gubens; Suresh S. Ramalingam; Enriqueta Felip; Jonathan W. Goldman; Cathie Scalzo; Erin Jensen; Debra A. Kush; and Rina Hui EBGMDHNARECNBLM-JAJPEASBC. Five-Year Overall Survival for Patients With Advanced Non–Small-Cell Lung Cancer Treated With Pembrolizumab: Results From the Phase I KEYNOTE-001 Study. *J Clin Oncol* 2019;37:2518–2527.
37. Martin Reck DRı-A, Andrew G. Robinson, Rina Hui, MBBS, Tibor Csoszi, Andrea Fu¨lo¨p; Maya Gottfried; Nir Peled; Ali Tafreshi; Sinead Cuffe; Mary O'Brien; Suman Rao; Katsuyuki Hotta; Kristel Vandormael; Antonio Riccio; Jing Yang; M. Catherine Pietanza; and Julie R. Brahmer. Updated Analysis of KEYNOTE-024: Pembrolizumab Versus Platinum-Based Chemotherapy for Advanced Non–Small-Cell Lung Cancer With PD-L1 Tumor Proportion Score of 50% or Greater. *Journal of clinical oncology* 2019;37:537–546.
38. Mok TSK, Wu YL, Kudaba I, et al. Pembrolizumab versus chemotherapy for previously untreated, PD-L1-expressing, locally advanced or metastatic non-small-cell lung cancer (KEYNOTE-042): a

randomised, open-label, controlled, phase 3 trial. Lancet 2019;393:1819–1830.

39. Ott PA, Bang YJ, Piha-Paul SA, et al. T-Cell-Inflamed Gene-Expression Profile, Programmed Death Ligand 1 Expression, and Tumor Mutational Burden Predict Efficacy in Patients Treated With Pembrolizumab Across 20 Cancers: KEYNOTE-028. J Clin Oncol 2019;37:318–327.
40. Samstein RM, Lee CH, Shoushtari AN, et al. Tumor mutational load predicts survival after immunotherapy across multiple cancer types. Nat Genet 2019;51:202–206.
41. Chan TA, Yarchoan M, Jaffee E, et al. Development of tumor mutation burden as an immunotherapy biomarker: utility for the oncology clinic. Ann Oncol 2019;30:44–56.
42. Luchini C, Bibeau F, Ligtenberg MJL, et al. ESMO recommendations on microsatellite instability testing for immunotherapy in cancer, and its relationship with PD-1/PD-L1 expression and tumour mutational burden: a systematic review-based approach. Ann Oncol 2019;30:1232–1243.
43. Palmeri M, Mehnert J, Silk AW, et al. Real-world application of tumor mutational burden-high (TMB-high) and microsatellite instability (MSI) confirms their utility as immunotherapy biomarkers. ESMO Open 2022;7:100336.
44. Donnem T, Kilvaer TK, Andersen S, et al. Strategies for clinical implementation of TNM-Immunoscore in resected nonsmall-cell lung cancer. Ann Oncol 2016;27:225–232.
45. Geng Y, Shao Y, He W, et al. Prognostic Role of Tumor-Infiltrating Lymphocytes in Lung Cancer: a Meta-Analysis. Cell Physiol Biochem 2015;37:1560–1571.
46. Zeng DQ, Yu YF, Ou QY, et al. Prognostic and predictive value of tumor-infiltrating lymphocytes for clinical therapeutic research in patients with non-small cell lung cancer. Oncotarget 2016;7:13765–13781.
47. Brambilla E, Le Teuff G, Marguet S, et al. Prognostic Effect of Tumor Lymphocytic Infiltration in Resectable Non-Small-Cell Lung Cancer. J Clin Oncol 2016;34:1223–1230.
48. Hargadon KM, Gyorffy B, McGee TJ. Genomic and transcriptional changes in IFNgamma pathway genes are putative biomarkers of response to ipilimumab immunotherapy in melanoma patients. Expert Rev Clin Immunol 2020;16:1099–1103.
49. Higgs BW, Morehouse CA, Streicher K, et al. Interferon Gamma Messenger RNA Signature in Tumor Biopsies Predicts Outcomes in Patients with Non-Small Cell Lung Carcinoma or Urothelial Cancer Treated with Durvalumab. Clin Cancer Res 2018;24:3857–3866.
50. Ready N, Hellmann MD, Awad MM, et al. First-Line Nivolumab Plus Ipilimumab in Advanced Non-Small-Cell Lung Cancer (CheckMate 568): Outcomes by Programmed Death Ligand 1 and Tumor Mutational Burden as Biomarkers. J Clin Oncol 2019;37:992–1000.
51. Bylicki O, Barazzutti H, Paleiron N, et al. First-Line Treatment of Non-Small-Cell Lung Cancer (NSCLC) with Immune Checkpoint Inhibitors. BioDrugs 2019;33:159–171.
52. Van TM, Blank CU. A user's perspective on GeoMxTM digital spatial profiling. Immuno-Oncology Technology 2019;1:11–18.

53. Gupta S, Zugazagoitia J, Martinez-Morilla S, et al. Digital quantitative assessment of PD-L1 using digital spatial profiling. Lab Invest 2020;100:1311–1317.
54. Zugazagoitia J, Gupta S, Liu Y, et al. Biomarkers Associated with Beneficial PD-1 Checkpoint Blockade in Non-Small Cell Lung Cancer (NSCLC) Identified Using High-Plex Digital Spatial Profiling. Clin Cancer Res 2020;26:4360–4368.
55. Toki MI, Merritt CR, Wong PF, et al. High-Plex Predictive Marker Discovery for Melanoma Immunotherapy-Treated Patients Using Digital Spatial Profiling. Clin Cancer Res 2019;25:5503–5512.
56. Valkenburg KC, de Groot AE, Pienta KJ. Targeting the tumour stroma to improve cancer therapy. Nat Rev Clin Oncol 2018;15:366–381.
57. Hellmann MD, Ciuleanu TE, Pluzanski A, et al. Nivolumab plus Ipilimumab in Lung Cancer with a High Tumor Mutational Burden. N Engl J Med 2018;378:2093–2104.

Tables

Tables 1 and 2 are available in the Supplementary Files section.

Figures

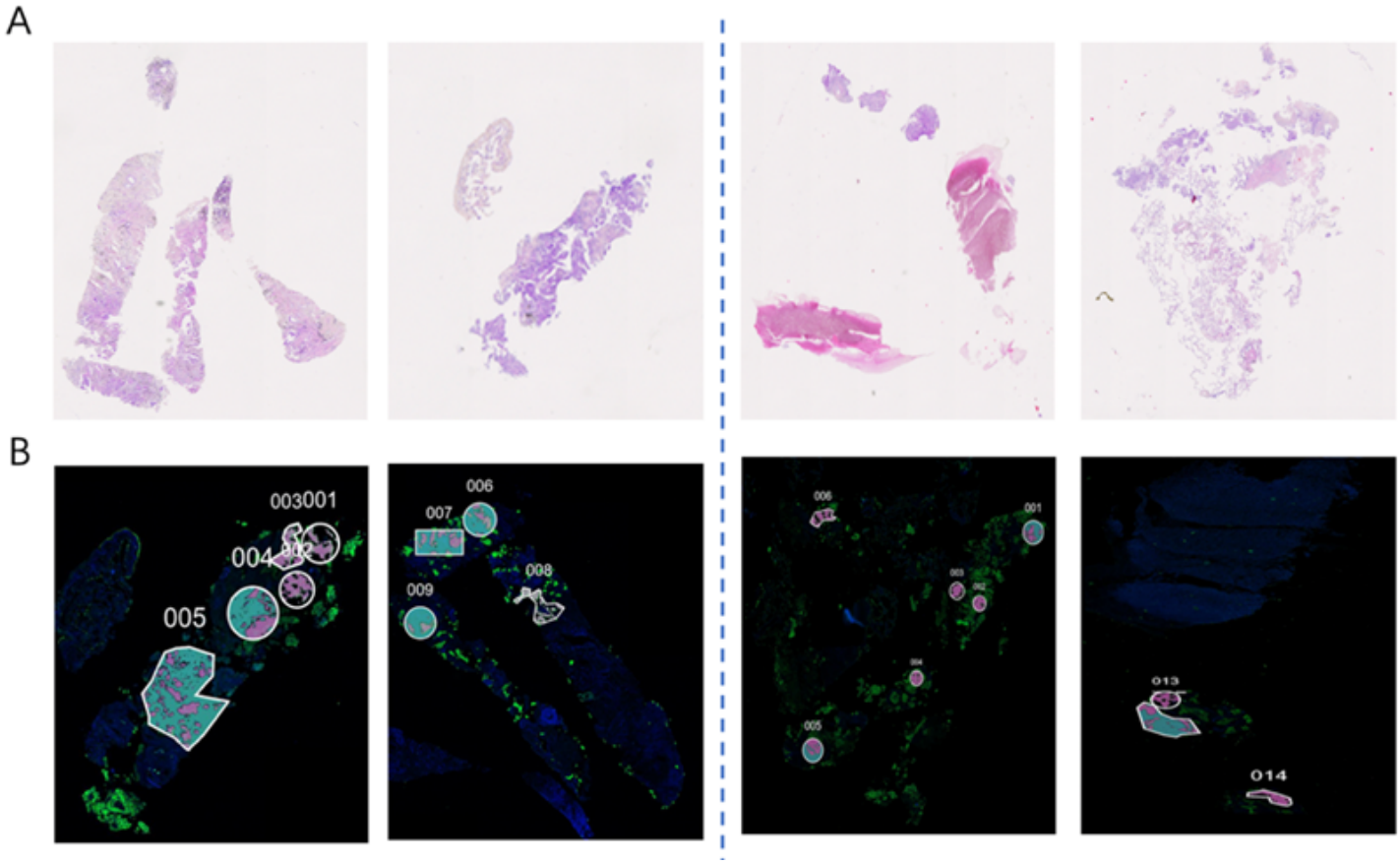

Figure 1

Representative hematoxylin-eosin (HE) staining images and regions of interest (ROIs) from patients in partial response (PR) and progressive disease (PD) group. (A) Representative HE images of advanced NSCLC patients before threated with KN046; (B) Representative ROI selection images from GeoMx Digital Spatial Profiling instrument.

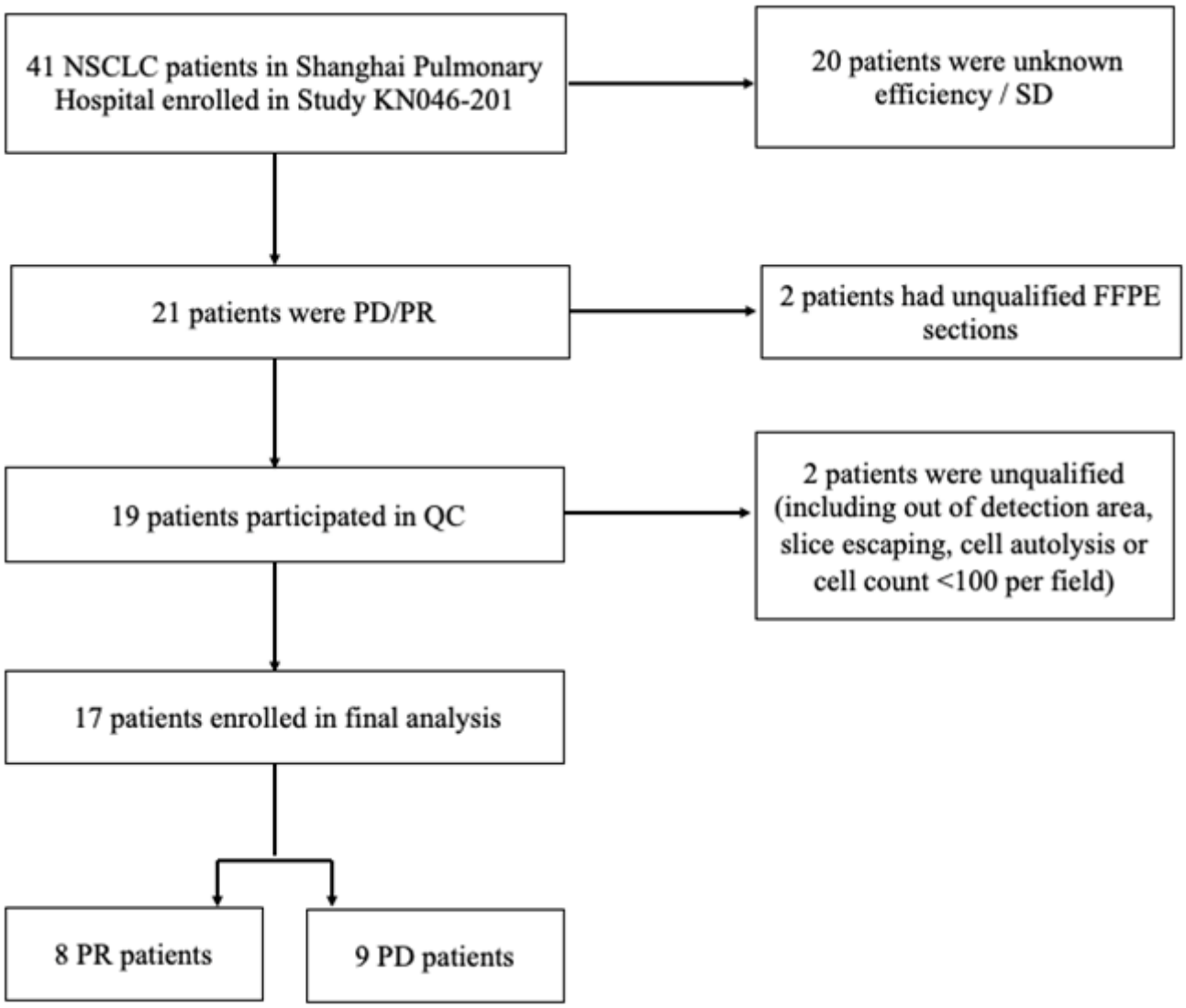

Figure 2

Flowchart of cohort with KN046.

NSCLC, non-small-cell lung cancer; SD, stable disease; PD, progressive disease; PR, partial disease; FFPE, formalin fixation and paraffin embedding; QC, Quality Control.

Figure 3

Different protein expression.

(A) According to response, heat map of all detected proteins in 2 groups. (B) Different protein expression between PR and PD groups of ROIs in all areas. (C) Different protein expression between 2 groups in tumor cell enriched areas. (D) Different protein expression between 2 groups in stroma areas.

Figure 4

Predictive effect of signatures from different areas.

(A) Heat map of different protein expression in all areas. (B) Boxplot of tumor + stroma signature in 2 groups. (C) ROC curve of tumor + stroma signature. (D) Heat map of different protein expression in tumor areas. (E) Boxplot of tumor signature in 2 groups. (F) ROC curve of tumor signature. (G) Heat map of different protein expression in stroma areas. (H) Boxplot of stroma signature in 2 groups. (I) ROC curve of stroma signature.

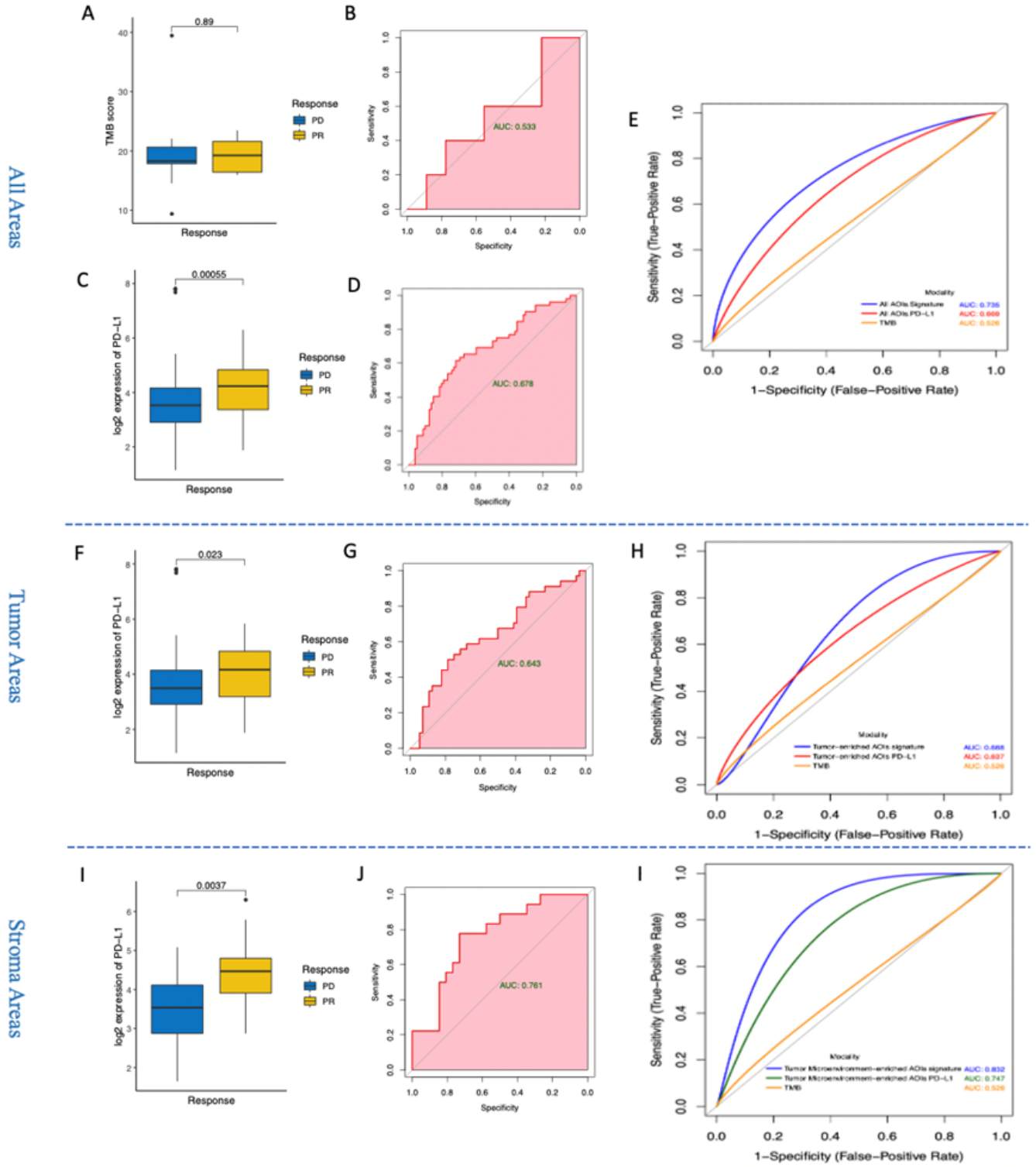

Figure 5

Compared with traditional makers.

(A) Boxplot of TMB (no partition defined). (B) ROC curve of TMB. (C) Boxplot of PD-L1 in all areas. (D) ROC curve of PD-L1 in all areas. (E) The meta-graph of 3 biomarkers' AUC value in all areas. (F) Boxplot of PD-L1 in tumor areas. (G) ROC curve of PD-L1 in tumor areas. (H) The meta-graph of 3 biomarkers'

AUC value in tumor areas. (I) Boxplot of PD-L1 in stroma areas. (J) ROC curve of PD-L1 in stroma areas. (K) The meta-graph of 3 biomarkers' AUC value in stroma areas.

Note: The meta-graphs showed smooth curves while the monographs showed broken lines which lead to the AUC values in meta-graphs were slightly different from those in AUC monographs.

Supplementary Files

This is a list of supplementary files associated with this preprint. Click to download.

- Tables.docx
- SuppFig1.png